Journal of Biological Engineering

RESEARCH

Open Access

Phenolic-loaded nanofiber from *Arctium lappa* root: a potential therapy for testosterone-induced ovarian oxidative stress

Viana Khojasteh[1], Seyed Amirmohammad Mollanorouzi[1], Ehsan Karimi[1*], Behrouz Ghorani[2] and Ehsan Oskoueian[1,3*]

Abstract

Polycystic Ovary Syndrome (PCOS) is a hormonal disorder affecting women of reproductive age, often associated with oxidative stress and inflammation. This study explores the therapeutic potential of *Arctium lappa* phenolic-rich fraction encapsulated nanofiber (ALPRF-NF) in a testosterone-induced PCOS mouse model. All experiments were performed in triplicate and Duncan's Multiple Range Test was used to assess significant differences between means, with significance determined at $p < 0.05$. The ALPRF-NF formulation demonstrated favorable physicochemical properties, including a ribbon-like structure (216.9 nm), a zeta potential of -19.3 mV, and a high encapsulation efficiency (93.1%). In vivo findings showed that ALPRF-NF significantly improved body weight, feed intake, and liver enzyme profiles in PCOS-induced mice ($p \leq 0.05$). It also enhanced the antioxidant defense system by elevating levels of glutathione peroxidase (GPX), superoxide dismutase (SOD), and catalase (CAT). Mechanistically, ALPRF-NF reduced oxidative stress and inflammation by delivering phenolic compounds that scavenge reactive oxygen species (ROS) and modulate gene expression in ovarian tissue. This included downregulation of inducible nitric oxide synthase (iNOS) and upregulation of SOD expression. These results suggest that ALPRF-NF effectively mitigates testosterone-induced ovarian oxidative damage and inflammation, offering a targeted, nanotechnology-based therapeutic approach for PCOS. The study provides valuable insights into novel strategies for improving women's reproductive health through bioactive compound delivery.

Keywords Nanomedicine, Drug delivery, Encapsulation, Polycystic ovary syndrome

Introduction

Ovarian inflammation, characterized by the dysregulation of inflammatory mediators and immune responses, is a common pathological condition associated with various disorders such as polycystic ovary syndrome (PCOS) and endometriosis [1]. Emerging evidence suggests that testosterone, a key androgen hormone, plays a significant role in the development and progression of ovarian inflammation. Therefore, identifying effective therapeutic approaches for mitigating testosterone-induced ovarian inflammation is of great importance [2].

Medicinal plants have been used for centuries in traditional medicine systems worldwide, and they continue to

*Correspondence:
Ehsan Karimi
ehskarimi59@iau.ac.ir
Ehsan Oskoueian
e.okoueian@gmail.com
[1]Department of Biology, Ma. C., Islamic Azad University, Mashhad, Iran
[2]Department of Food Nanotechnology, Research Institute of Food Science and Technology (RIFST), km 12 Mashhad-Quchan Highway, Mashhad, Iran
[3]Department of Research and Development, Arka Industrial Cluster, Mashhad, Iran

play a significant role in modern medicine [3]. They offer a rich source of bioactive compounds, including phenolic compounds, flavonoids, alkaloids, and terpenoids, which possess diverse pharmacological properties [4]. These compounds exhibit anti-inflammatory, antioxidant, immunomodulatory, and antimicrobial activities, making them promising candidates for the treatment of inflammatory conditions [5]. One of the key advantages of medicinal plants is their relatively lower incidence of side effects compared to synthetic drugs [6]. Natural bioactive compounds derived from medicinal plants often exhibit a higher degree of compatibility with the human body due to their evolutionarily conserved interactions. As a result, they are generally well-tolerated and have a reduced risk of adverse effects [7, 8].

Arctium lappa (Asteraceae), commonly known as burdock, is a medicinal plant with a long history of traditional use in various cultures for its potential health benefits [9, 10]. The root of *A. lappa* is particularly rich in phenolic compounds, known for their potent antioxidant and anti-inflammatory properties [11].

Nanotechnology encompasses the areas of science and engineering that concentrate on phenomena at the nanoscale, focusing on the design, characterization, production, and application of materials, structures, devices, and systems [12, 13]. This technology has the capacity to transform medical research and introduce a new phase of human enhancement [14, 15]. There is substantial potential for nanotechnology in diagnostic, therapeutic, and preventive roles [16]. This cutting-edge approach enables deliberate alterations to the body to tackle various health challenges. The application of nanoparticle-based medications has demonstrated improvements in bioavailability, a decrease in side effects, and better absorption of therapeutic agents [17].

In recent years, nanofiber-based drug delivery systems have emerged as a promising technology for the targeted and controlled delivery of bioactive compounds [18]. Nanofibers are nanoscale fibers with a high surface area-to-volume ratio, which allows for efficient encapsulation and delivery of therapeutic agents [19]. They can be fabricated from a wide range of materials, including natural polymers, synthetic polymers, and composite materials. Natural polymers, such as proteins and polysaccharides, are particularly attractive for the development of nanofibers due to their biocompatibility, biodegradability, and availability from renewable sources [20, 21].

The utilization of nanofibers as a delivery vehicle offers several advantages, including increased surface area, improved stability of encapsulated compounds, sustained release kinetics, and enhanced penetration into target tissues [21]. Furthermore, the incorporation of phenolic compounds of *A. lappa* root into nanofibers holds the potential to harness their anti-inflammatory properties and facilitate their precise delivery to the inflamed ovarian tissues.

The objective of this study is to investigate the therapeutic efficacy of phenolic compound-loaded nanofibers of *A. lappa* root in mitigating testosterone-induced ovarian inflammation in an experimental animal model. Through comprehensive in vivo assessments, we aim to evaluate the anti-inflammatory effects of these nanofibers, elucidate their underlying mechanisms of action, and explore their potential as a novel therapeutic approach for ovarian inflammation management.

Materials and methods

Plant material and chemicals

The root of *Arctium lappa* was procured from the Mashhad Herbal Medicine Market situated in Iran. A voucher specimen was deposited at the Sari Agricultural Sciences and Natural Resources University (SANRU) herbarium under the code SANRU-H1051. Zein powder derived from corn (Z 3625, 22–24 kDa, possessing a total protein concentration of 98%) was sourced from Sigma-Aldrich (Madrid, Spain), while glacial acetic acid (99.7%) was acquired from Molekula (England). Female Balb/c mice were obtained from the Serum Research Institute in Mashhad. RNA extraction and cDNA synthesis kits, alongside SYBR Green master mix, were purchased from Biofact Company in Korea. All remaining materials and reagents not explicitly specified herein were procured from Daejung (Siheung, Korea).

Phenolic compounds fractionation protocol

The *A. Lappa* root was subjected to grinding to obtain a fine powder using a grinder mill. A mixture comprising 100 g of the dried powder, 900 mL of aqueous methanol (80% (v/v)), and 100 mL of 6 M HCl underwent extraction via the reflux [22]. The resulting extract was evaporated at 60 °C and fractionation was conducted using separating funnel with the help of various polarity solvents including hexane, chloroform, ethyl acetate, n-butanol, and water [23]. Subsequent to fractionation, the supernatant was filtered and total phenolic compounds (TPC) in each fraction were determined by mixing 0.1 ml of the extract, 2.5 ml of Folin-Ciocalteu reagent (1:10 v/v), and 2 ml of 7.5% sodium carbonate in a test tube covered with aluminum foil. After vortexing, the absorbance was measured at 765 nm [23].

Synthesized of nanofiber-encapsulated PRF

The electrospinning solutions were prepared by dissolving zein powder in a solution of 80% ethanol at concentrations of 20%, 25%, 30%, 35%, and 40% w/v. The solutions were vigorously stirred at 300 rpm for an hour until a completely clear solution was obtained. To ensure ideal spinnability, a solution should be free from needle

blockages, possess uniform fiber morphology, and be free from beads-on-a-string or "spindle" defects. A solution's suitability was determined by its inability to form a gel, as high-viscosity solutions hinder the electrospinning process [24].

We encapsulated PRF of *A. Lappa* at concentrations of 1%, 2%, 3%, and 4% (w/w) in the above solution. After mixing the solutions with PRF of *A. Lappa* for 30 min at room temperature, they were subjected to high voltage. PRF-loaded zein nanofibers were produced using a high-voltage electrospinning apparatus (Electrospinning Starter Kit-Yflow, Spain). The electrospinning was carried out using a plastic syringe fitted with a stainless-steel needle (Sigma-Aldrich, inner diameter = 0.838 mm, outer diameter = 1.270 mm, and 18 gauge) discharged into the collector (100 × 100 mm2 flat plate collector of stainless steel) under a voltage of 25 kV, a flow rate of 0.2 ml/h, and 150 mm tip-to-collector distance. The electrospinning was performed under ambient conditions of 25 °C, 23% RH, for 60 min. A square aluminum foil target measuring 100*100 mm^2, mounted on an earthed copper plate, was supported by two polypropylene blocks [24].

Physicochemical attributes of ALPRF-NF

The ALPRF-NF sample was diluted 20-fold in water to prepare it for biophysical analysis. Dynamic light scattering (DLS) was performed on the diluted ALPRF-NF solution to measure the zeta potential of any particles present. Zeta potential provides insight into surface charge, an important factor influencing particle stability. Additionally, field emission scanning electron microscopy (FESEM) was used to directly observe nanoscale morphologies and quantify size dimensions within the sample. FESEM allows high-resolution imaging at the nanometer scale. Both DLS and FESEM analyses were conducted using a Malvern Zetasizer Nano ZS instrument. Measurements for zeta potential determination via DLS were repeated three times to obtain an average value.

To calculate the encapsulation efficiency (EE) of PRF of *A. Lappa* in nanofiber, follow the steps below. First, take 50 mg of electrospun fiber and submerge it in 10 mL of heptane. Then, shake the mixture for 15 min at 100 rpm. After that, filter the mixture and measure the absorbance at 250 nm using UV-1800 from Shimadzu, Japan. You can then analyze the mixture. To determine the amount of PEF present in the nanofibers, refer to a calibration curve ($R^2 = 0.99$) prepared by dissolving various quantities of PEF in heptane. Finally, calculate the EE value using the following formula [23]:

$$\text{Encapsulation efficiency}(\%) = \frac{weight\ of\ the\ PRF\ in\ nanoparticles}{weight\ of\ the\ feeding\ PRF - NF} \times 100$$

Phytochemical screening of ALPRF-NF using HPLC

We conducted an RP-HPLC analysis to examine the phenolic profiling of nanofiber-loaded PRF of *A. Lappa*, following the methods described by Oskoueian et al. [23]. We used two solvents, A (deionized water) and B (acetonitrile), for analysis. The column was equilibrated using 85% solvent A and 15% solvent B for 15 min. We increased the proportion of solvent B to 85% at the 50th minute and decreased it to 15% at minute 55, maintaining this ratio for an hour for the subsequent analysis at a flow rate of 0.6 ml/min. The phenolic standards considered in this study were gallic acid, syringic acid, vanillic acid, salicylic acid, caffeic acid, pyrogallol, catechin, cinnamic acid, chlorogenic acid, naringin, chrysin, and ferulic acid, as previously described [23].

Mice trial experiment

28 white female Balb/c mice weighing 30–35 g each were housed individually at 23 °C ± 1 °C and 58%±10% humidity. They adapted to the laboratory for 7 days with 12-hour light/dark cycles. The mice were fed a standard pellet diet from Javaneh Khorasan, Mashhad, Iran and had access to tap water. The mice were separated into four groups, with seven mice in each group. T1 was the control group, while PCOS-like symptoms were induced in the other three groups by subcutaneously injecting testosterone enanthate (TE) at 1 mg/kg in the back of their necks for 60 days. After 4 weeks of TE injection, Group II received a normal diet, while Group III and Group IV received a ALPRF-NF and Metformin respectively. At the end of the experiment, the mice were euthanized with pentobarbital-HCL at a dose of 50 mg/kg, i.p. blood, liver, and ovarian tissues were collected immediately for liver enzyme analysis, lipid peroxidation assay, and gene expression changes. Animal experiments approved by Ethics Committee of Islamic Azad University of Mashhad (Khorasan Razavi, Iran) with approval number IR.IAU.MSHD.REC.1402.002.

Haematological and lipid peroxidation evaluation

Liver enzymes such as aspartate aminotransferase (AST), alanine transaminase (ALT), and alkaline phosphatase (ALP), as well as antioxidant markers like glutathione peroxidase (GPX) and superoxide dismutase (SOD), and hormones such as insulin, luteinizing hormone (LH), and follicle-stimulating hormone (FSH) were measured using an auto-analyzer (Hitachi 902, Japan) and biochemical kits. To test for lipid peroxidation in the ovarian, the tissues were homogenized and mixed with distilled water, BHT, sodium dodecyl sulfate, and TBA. The solution was heated and then cooled before being shaken with n-butanol and centrifuged. The absorbance was read and the results were analyzed as a percentage relative to the control [25].

Ovarian and liver histopathology

Histopathological examination of the liver and ovaries was conducted to assess any potential structural changes. After euthanizing the mice, the livers and ovaries were carefully washed with normal saline solution. Subsequently, the isolated organs were fixed in a 10% buffered formalin solution, prepared in 0.1 M sodium phosphate buffer with a pH of 7. The preserved organs were then processed for paraffin embedding, followed by sections for staining purposes. The staining protocol employed was based on the method described by Moshfegh et al. [26] utilizing a hematoxylin and eosin staining protocol. Meanwhile, the ovarian morphometric features including primordial follicle diameter, primary follicle diameter, per-antral follicle diameter, and antral follicle diameter were assessed.

Gene analysis confirmation

To investigate the underlying molecular mechanism of action of ALPRF-NF in ovarian tissues, we focused on assessing the expression of key antioxidant and inflammatory genes, specifically iNOS and SOD. Ovarian tissue samples were promptly frozen in liquid nitrogen upon collection to preserve their molecular integrity. Subsequently, Frozen tissues were pulverized with liquid nitrogen and a mortar and pestle for RNA extraction using a specialized kit. Following extraction, cDNA libraries were generated using a cDNA synthesis kit. For gene expression analysis, a set of specific primer sequences (listed in Table 1) were employed to quantify the expression levels of the target genes, with beta-actin serving as the reference gene for normalization. Notably, a comparative quantitative polymerase chain reaction (qPCR) utilizing SYBR Green PCR Master Mix (Roche Diagnostics) was employed. The qPCR amplification protocol involved an initial denaturation step at 95 °C for 5 min (1X), followed by 35 cycles of denaturation at 95 °C for 20 s, annealing at 56 °C for 25 s, and extension at 72 °C for 30 s [26].

Data analysis procedures

The experimental procedures were conducted in triplicates to ensure the robustness and reliability of the results. The statistical analysis of the obtained data was expressed as means accompanied by their corresponding standard deviations (SD) to provide a measure of variability. To determine the significance of the differences between the means, we employed Duncan's Multiple Range Test. The significance level was set at $p < 0.05$, indicating a statistically significant difference if the obtained p-value was less than 0.05.

Table 1 The primer sets of targeted genes

Gene	Forward (5′ to 3′)	Reverse (3′ to 5′)
SOD	GTCGGCTTCTCGTCTTGCTC	GCTTTCATCGCCATGCTTCC
iNOS	CACCTTGGAGTTCACCCAGT	ACCACTCGTACTTGGGATGC
β-actin	CCTGAACCCTAAGGCCAACC	CAGCTGTGGTGGTGAAGCTG

Results and discussion

Analysis of phenolic compound fractionation

According to the analysis conducted on the fractionation, it was found that ethyl acetate contains the highest amount of phenolic content at 227 mg/kg. The subsequent compounds in descending order were n-butanol at 152 mg/kg, water at 103 mg/kg, chloroform at 71 mg/kg and hexane at 36 mg/kg GAE/g DW. Due to the higher concentration of phenolic compounds, ethyl acetate was chosen as the ideal candidate for encapsulation in zein nanofibers. Comparing these results with previous studies, it is crucial to consider variations in extraction methods, sample composition, and analytical techniques [27]. Studies investigating phenolic content in similar samples have reported varying concentrations depending on the extraction solvents and analytical methods employed [28]. For instance, study have been carried out by Nurcholis et al. [29] reported higher phenolic content in ethyl acetate extract compared to our findings, indicating potential variations in the phenolic composition of the samples. Conversely, Deghima et al. [30] reported lower phenolic content in n-butanol extract, suggesting differences in the extraction efficiency of phenolic compounds. Furthermore, the choice of solvents for phenolic extraction depends on the polarity of the compounds of interest. Ethyl acetate, being a moderately polar solvent, is generally effective in extracting a wide range of phenolic compounds. However, other solvents such as methanol, ethanol, or acetone may yield different results due to their varying polarities and selectivity towards specific phenolic compounds [30, 31].

Characterization and encapsulation efficiency analysis

The importance of DLS in the encapsulation of phenolic compounds lies in its ability to provide critical information about the size distribution, stability, and colloidal properties of nanofibers, thereby facilitating the development of efficient and reliable encapsulation strategies for harnessing the therapeutic potential of phenolic compounds [32]. Figures (1**A**) demonstrates the results of the dynamic light scattering technique indicating particles with an average size of 216.93 nm. The PDI of ALPRF-NF was shown to be 0.32, which was in the acceptable range. Examining the zeta potential of nanoparticles demonstrated that the ALPRF-NF has a negative zeta potential with values of -19.3 mV (Fig. 1B), which indicates the formation of particles with high stability. The electron microscope examination of synthesized nanofiber exhibited uniform ribbon-like morphology without spheres confirmed particles with uniform dispersion (Fig. 1C).

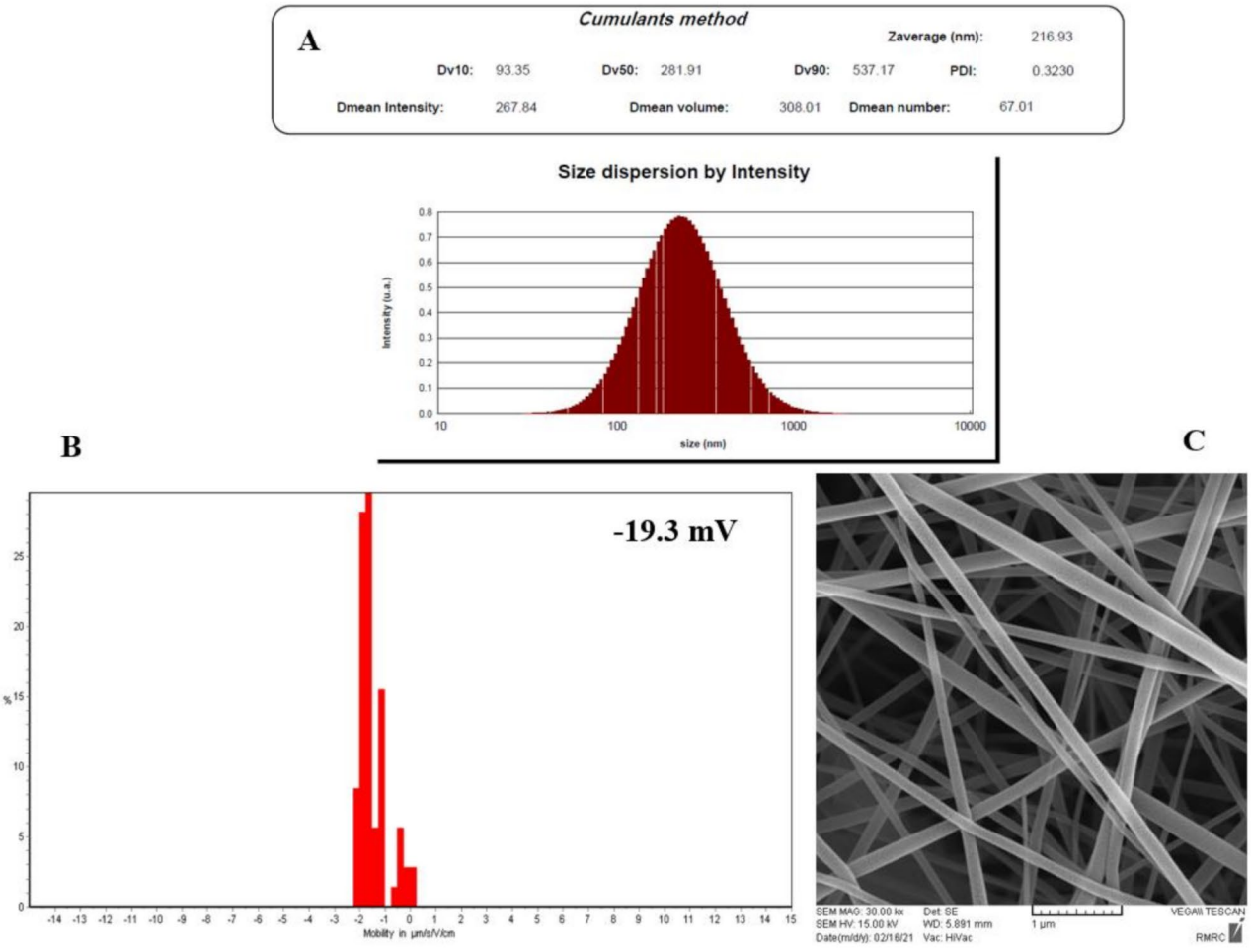

Fig. 1 Physicochemical characteristics of ALPRF-NF, DLS (**A**), zeta potential (**B**) and FESEM micrograph (**C**)

Table 2 Phenolic profiling presented in the ALPRF-NF

Phenolic compounds contents (µg/g DW)				
Gallic acid	**Caffeic acid**	**Chlorogenic acid**	**Syringic acid**	**Naringin**
211.4 ± 6.3	285 ± 4.9	302 ± 5.6	805 ± 8.2	788 ± 4.1

The analyses were performed in triplicates

Furthermore, the encapsulation efficiency of the PRF was calculated to be 93.1%.

Phenolic compounds profiling of ALPRF-NF

Based on the RP-HPLC analysis, ALPRF-NF contains numerous bioactive compounds including gallic acid, caffeic acid, chlorogenic acid, syringic acid and naringin ranging from 211.4 to 805.8 µg/g DW (Table 2). Syringic acid and naringin are the most abundant phenolic compounds, with values of 805.8 and 788.4 µg/g DW, respectively, compared to other standards. These findings are consistent with Luquis et al. [33], who demonstrated that *A. lappa* leaves contain chlorogenic acid, cafeic acid, and p-coumaric acid. These results are also in line with several studies [34–36], who reported the presence of flavonoids, phenolic acids, and lignans in *Arctium lappa* L seed.

Body weight and food intake alteration

During the experiment, the control group mice gained an average of 57.85 mg of weight per day (T1). However, the mice with PCOS induced by testosterone showed a significant decrease in weight gain (T2), as shown in Table 3. When the mice were given ALPRF-NF supplements (T3) and metformin (T4), their weight gain significantly increased ($p < 0.05$). The mice's appetite was directly proportional to the changes in their weight gain (Table 3). The mice that received the ALPRF-NF-supplemented regimen showed an increase in appetite ($p > 0.05$), leading to an increase in food intake. On the other hand, the PCOS-induced mice supplement with normal food (T2) showed a decrease in food consumption. Based on the results, the mice in the ALPRF-NF-treated group consumed the most food ($p < 0.05$), while the PCOS-injected mice (T2) were less inclined to consume food compared to others, as presented in Table 3. The study found that

Table 3 The average daily weight gain and average daily feed intake in mice receiving different treatments

Average	T1	T2	T3	T4	SEM
Average daily weight gain (mg/day)	57.85[c]	41.78[d]	92.5[a]	79.28[b]	6.62
Average daily feed intake (g/day)	5.04[a]	4.58[b]	5.26[a]	4.69[b]	1.83

T1: Control

T2: Testosterone-induced PCOS mice + normal food

T3: Testosterone-induced PCOS mice + nanofiber

T4: Testosterone-induced PCOS mice + metformin

Different letters in the same row indicated significant differences ($p < 0.05$)

The analyses were performed in triplicates

Table 4 The liver enzyme, antioxidant and hormone content in mice receiving different treatments

Treatment	AST (U/L)	ALT (U/L)	ALP (U/L)	SOD (U/ml)	GPX (U/ml)	Insulin (Iu/L)	LH (Iu/L)	FSH (Iu/L)	Es (Pg/ml)	Glu (mg/dl)
T1	46[b]	165[b]	487[d]	55[b]	371[b]	5.1[d]	12.3[c]	26.2[a]	29.5[d]	260[a]
T2	52[a]	191[a]	789[a]	42[d]	225[d]	11.2[a]	17.3[a]	19.8[c]	43.5[a]	199[c]
T3	41[c]	136[d]	702[c]	63[a]	402[a]	8.5[b]	14.2[b]	21.4[b]	34.8[c]	219[b]
T4	44[b]	151[c]	721[b]	48[c]	276[c]	7.2[c]	16.5[a]	22.1[b]	39.1[b]	192[d]
SEM	2.11	4.60	7.32	4.11	9.72	0.68	2.14	0.59	2.37	3.48

T1: Control

T2: Testosterone-induced PCOS mice + normal food

T3: Testosterone-induced PCOS mice + nanofiber

T4: Testosterone-induced PCOS mice + metformin

Different letters in the same raw indicated significant difference ($p < 0.05$)

The analyses were performed in triplicates

ALPRF-NF had a greater effect on the mice's appetite than metformin, possibly due to the use of nanofibers as a drug delivery system for *A. lappa* phenolic-rich fraction.

Analysis of blood and hormone levels

The study found that there were significant differences in liver enzyme levels between the treatment groups. Specifically, the mice in group T2, which were induced with testosterone to develop polycystic ovary syndrome (PCOS), had significantly higher levels of the AST and ALT enzymes, indicating liver damage. However, groups T3 and T4, which received ALPRF-NF and metformin, respectively, had significantly lower levels of AST and ALT, suggesting a protective effect on liver function (Table 4).

The mice in group T2 also had significantly higher levels of ALP, another liver enzyme, compared to the control group. This indicates liver injury due to testosterone induction. However, groups T3 and T4 had significantly lower levels of ALP, suggesting a protective effect against liver damage.

Supplementation with ALPRF-NF in group T4 resulted in the highest levels of the antioxidant defense mechanisms glutathione peroxidase (GPX), superoxide dismutase (SOD), and catalase (CAT) among all the treatment groups (Table 4).

The mice with Testosterone-induced PCOS that received normal food (T2) exhibited a significant increase in insulin, luteinizing hormone (LH), and estradiol levels, as well as a decrease in follicle-stimulating hormone (FSH) and glucose content compared to the normal control group. However, groups T3 and T4 demonstrated a significant reduction in insulin, LH, and estradiol levels, as well as an improvement in FSH and glucose content compared to the control group. Based on the results presented in Table 4, ALPRF-NF significantly modulated all factors such as liver enzymes, antioxidant power, and hormone levels in mice induced with PCOS compared to the synthetic drug metformin. A study conducted by moshfegh et al. [26] evaluated the effects of saffron petal extract (SPE) and saffron petal anthocyanins (SPA) on ovarian hormones and steroidogenic enzymes. The results showed that following SPE and SPA treatment significantly enhance the antioxidant levels ($P < 0.01$).

Ovarian lipid peroxidation analysis

As presented in Fig. 2, an escalation in malondialdehyde (MDA) levels was observed in mice inducing polycystic ovary syndrome (PCOS) when they were fed a normal diet (T2), as compared to the control group (T1). However, the administration of ALPRF-NF (T3) exhibited a significant ($p < 0.05$) mitigation of the rise in MDA levels within ovarian tissue, indicating a dose-dependent reduction (Fig. 2). Malondialdehyde (MDA) is a well-established biomarker widely used to assess oxidative stress in various pathological conditions [37]. The observed increase in MDA levels in the subjects with polycystic ovary syndrome (PCOS) highlights the presence of

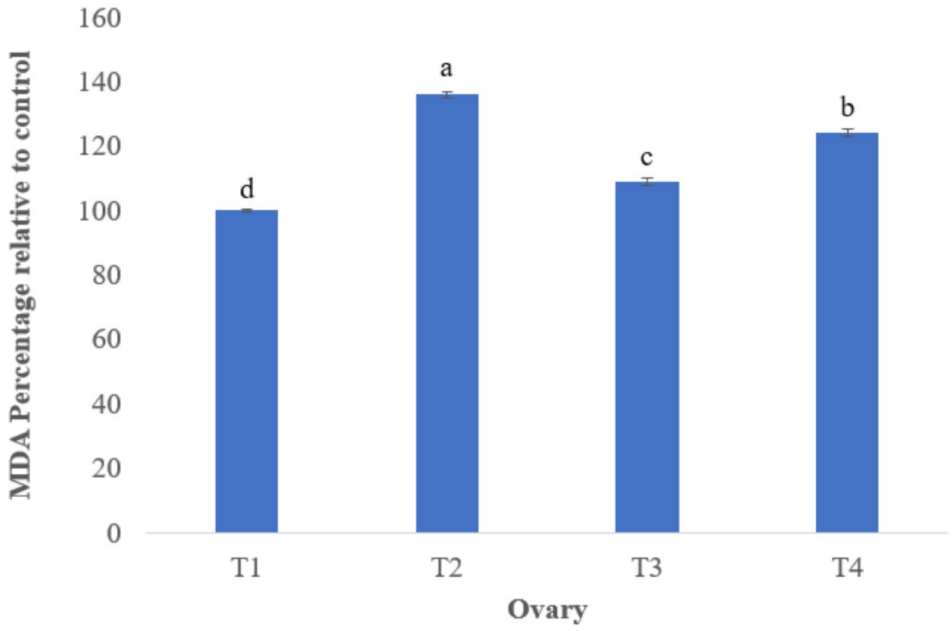

Fig. 2 The lipid peroxidation in the ovary of mice under different treatments; T1: Control, T2: Testosterone-induced PCOS mice + normal food, T3: Testosterone-induced PCOS mice + nanofiber, T4: Testosterone-induced PCOS mice + metformin, Different letters in the same raw indicated significant difference ($p < 0.05$), The analysis was performed in triplicates

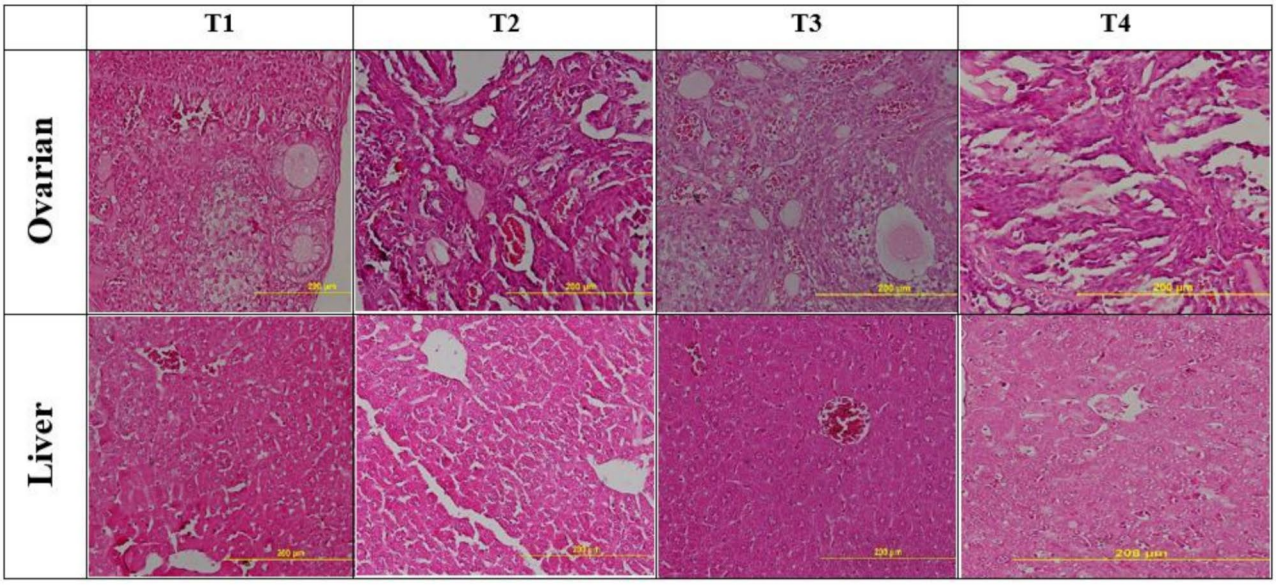

Fig. 3 The liver and ovary histopathology. T1: control, T2: Testosterone-induced PCOS mice + normal food, T3: Testosterone-induced PCOS mice + nanofiber, T4: Testosterone-induced PCOS mice + metformin

oxidative burden in these individuals. It is worth noting that lifestyle modifications and dietary interventions incorporating antioxidant-rich components have shown promising results in reducing the concentrations of oxidative stress biomarkers, including MDA [38, 39]. These interventions offer potential strategies to mitigate the detrimental effects of oxidative stress associated with PCOS [40].

Histopathological characteristics and morphometric analysis

In contrast to the control group, the mice-induced PCOS groups that received various treatments did not exhibit any significant histopathological changes in their liver and ovarian tissues, as depicted in Fig. 3. The morphometric analysis of the ovary, presented in Table 5, provides valuable insights. The results clearly indicate that

Table 5 Morphometric analysis of ovarian tissue of mice received different treatments

Treatment	Primordial Follicles Diameter (μm)	Primary Follicles Diameter (μm)	Per-antral Follicles Diameter (μm)	Antral Follicles Diameter (μm)
T1	51^{a}	96^{b}	187^{b}	245^{a}
T2	41^{d}	80^{d}	172^{c}	227^{c}
T3	46^{b}	104^{a}	231^{a}	239^{b}
T4	44^{c}	84^{c}	175^{c}	222^{c}
SEM	1.36	1.9	3.7	4.7

T1: control

T2: Testosterone-induced PCOS mice + normal food

T3: Testosterone-induced PCOS mice + nanofiber

T4: Testosterone-induced PCOS mice + metformin

Different letters in the same raw indicated significant differences ($p < 0.05$)

The analyses were performed in triplicates

Table 6 The expression analysis of antioxidant and inflammation-related genes in ovarian mice received different treatments

	T1	T2	T3	T4	SEM
Down-regulated gene					
Antioxidant-related genes					
SOD	1^{a}	-3.46^{d}	-2.24^{c}	-1.16^{b}	0.09
Up-regulated gene					
Inflammation-related gene					
iNOS	1^{c}	$+3.86^{a}$	$+2.16^{b}$	+1.76	0.12

T1: control; T2: Testosterone-induced PCOS mice + normal food; T3: Testosterone-induced PCOS mice + nanofiber; T4: Testosterone-induced PCOS mice + metformin

Different letters in the same raw indicated significant differences ($p < 0.05$)

The analyses were performed in triplicates

+: indicated up-regulation as compared to the control group (T1)

-: indicated down-regulation as compared to the control group (T1)

the group of mice induced with PCOS and fed a normal diet experienced a significant decrease in the diameter of primordial follicles, primary follicles, per-antral follicles, and antral follicles compared to the control group ($P < 0.05$). However, the consumption of ALPRF-NF notably enhanced these parameters ($P < 0.05$). The mechanism of action underlying the enhancement of these parameters by ALPRF-NF can be attributed to the antioxidant properties of various phenolic compounds encapsulated in nanofiber. Phenolic compounds are known to scavenge reactive oxygen species (ROS) and reduce oxidative stress within the ovarian tissue. By neutralizing ROS, phenolic compounds help to maintain the structure and integrity of the ovarian follicles, preventing their degeneration and promoting their growth. This antioxidant activity can contribute to the preservation and development of healthy follicles, ultimately leading to improved morphometric characteristics observed in the treated groups. Additionally, phenolic compounds may exert their effects through the modulation of signaling pathways involved in follicular development and maturation, although further research is needed to fully elucidate these mechanisms. Our findings align closely with a recent experimental study examining the impact of saffron petal extract (SPE) on ovarian histology in mice induced with testosterone. This investigation revealed a notable reduction in the number of cystic follicles following SPE intervention in mice exhibiting polycystic ovary syndrome (PCOS) induced by testosterone. Moreover, testosterone administration demonstrated efficacy in ameliorating PCOS-like symptoms, including an increase in corpus luteum and preovulatory follicle count [26]. Our findings align with the study conducted by Hu et al. which showed that the use of medicinal plants resulted in the successful induction of the syndrome and compromised follicular development in adult mice [41].

SOD and iNOS genes expression analyses

The expression analysis of key antioxidant (SOD) and inflammatory (iNOS) genes in ovarian tissue is detailed in Table 6. Our findings reveal that administration of ALPRF-NF significantly ($p < 0.05$) augmented the expression of the SOD gene. This up-regulation of SOD gene expression underscores the mitigation of oxidative stress within ovarian tissues, corroborating observations of reduced lipid peroxidation. Furthermore, our investigation demonstrates a noteworthy down-regulation of the iNOS gene following ALPRF-NF treatment, indicative of a pronounced attenuation of inflammation in testosterone-induced PCOS mice. These results underscore the potential of ALPRF-NF as a therapeutic intervention for mitigating both oxidative stress and inflammation, highlighting avenues for further elucidation of its mechanisms of action and clinical utility in PCOS management. The findings from our present investigation validate the outcomes of previous research, wherein it was demonstrated that treatment with saffron petal extract (SPA) leads to a reduction in TNF-α, IL-6, IL-1ß, and IL-18 inflammatory genes. Moreover, this treatment regimen reinstates the balance of NF-κB and IκB, pivotal regulators of inflammatory gene expression, in testosterone-induced mice [26]. Additionally, another study has reported a decrease in mRNA levels of inflammatory genes in polycystic ovary syndrome (PCOS) specimens upon treatment with compounds isolated from plants [42]. The therapeutic efficacy of ALPRF-NF in managing PCOS symptoms appears to be primarily mediated through its potent antioxidant and anti-inflammatory activities, attributed to the phenolic compounds encapsulated within the nanofiber matrix. Phenolic constituents such as syringic acid, naringin, caffeic acid, and chlorogenic acid are known to scavenge reactive oxygen species, thereby mitigating oxidative stress a key pathological hallmark in PCOS. The upregulation of superoxide dismutase and glutathione

peroxidase, coupled with the downregulation of inducible nitric oxide synthase, reflects a molecular shift towards an enhanced antioxidant defense and reduced inflammatory burden in ovarian tissues. Additionally, these phenolics may modulate endocrine function by influencing the hypothalamic-pituitary-ovarian axis, resulting in the normalization of key reproductive hormones such as LH, FSH, estradiol, and insulin. The nanofiber delivery system likely enhances the bioavailability and sustained release of these compounds, contributing to the observed improvements in follicular morphology, lipid peroxidation, and metabolic profiles.

Conclusion

This study highlights the therapeutic potential of *Arctium lappa* phenolic-rich fraction encapsulated nanofiber (ALPRF-NF) in managing testosterone-induced polycystic ovary syndrome (PCOS). ALPRF-NF treatment improved metabolic outcomes, enhanced antioxidant defense, and modulated key ovarian genes involved in oxidative stress and inflammation, such as iNOS and SOD. Despite these promising findings, the study's scope is limited to a preclinical mouse model, and its translatability to human applications remains to be validated. Further research is needed to investigate the long-term safety, mechanistic pathways, and clinical efficacy of ALPRF-NF. Future directions should also include dose optimization, bioavailability assessments, and exploration of synergistic effects with standard PCOS therapies. Overall, nanofiber-based delivery of plant-derived phenolics presents a promising approach for targeted, non-invasive interventions in women's reproductive health, particularly in addressing oxidative stress-related disorders such as PCOS.

Author contributions

VKH and SM: Study design, experimental work and writing original draft; EK, BGH and EO: analysis, methodology, project administration, supervision, review, and editing of the original draft; All authors read and approved the final manuscript.

Funding

Not applicable.

Data availability

No datasets were generated or analysed during the current study.

Declarations

Ethics approval and consent to participate

All animal handling methods were accomplished as per the Islamic Azad University of Mashhad, IRAN regulations with their prior approval for using the animals (IR.IAU.MSHD.REC. 1402.002). All methods and procedures were carried out in accordance with the relevant guidelines and regulations. All methods are reported in accordance with ARRIVE guidelines.

Competing interests

The authors declare no competing interests.

Received: 29 January 2025 / Accepted: 28 April 2025
Published online: 09 May 2025

References

1. Wang J, Yin T, Liu. Dysregulation Immune Response PCOS Organ Syst. 2023;14:1169232.
2. Wang D et al. *Exposure to hyperandrogen drives ovarian dysfunction and fibrosis by activating the NLRP3 inflammasome in mice.* 2020. 745: p. 141049.
3. Khan MI et al. Anticancer properties of medicinal plants and their bioactive compounds against breast cancer: a review on recent investigations. 2022. 29(17): pp. 24411–44.
4. Tungmunnithum D et al. *Flavonoids and other phenolic compounds from medicinal plants for pharmaceutical and medical aspects: An overview.* 2018. 5(3): p. 93.
5. Huang W-Y et al. *Natural phenolic compounds from medicinal herbs and dietary plants: potential use for cancer prevention.* 2009. 62(1): pp. 1–20.
6. Roleira FM et al. Phenolic derivatives from medicinal herbs and plant extracts: anticancer effects and synthetic approaches to modulate biological activity. 2018. 57: pp. 115–56.
7. Chavda VP et al. *Nano-drug delivery systems entrapping natural bioactive compounds for cancer: recent progress and future challenges.* 2022. 12: p. 867655.
8. Bishayee A, Sethi G. *Bioactive natural products In cancer prevention and therapy: progress and promise.* In *Seminars In cancer biology*. Elsevier; 2016.
9. de Souza ARC et al. Assessment of composition and biological activity of Arctium lappa leaves extracts obtained with pressurized liquid and supercritical CO2 extraction. 2019. 152: p. 104573.
10. de Souza ARC et al. Phytochemicals and biological activities of Burdock (Arctium Lappa L.) extracts: A review. 2022. 19(11): p. e202200615.
11. Petkova N et al. Phytochemical composition and antimicrobial properties of Burdock (Arctium Lappa L.) roots extracts. 2022. 12: pp. 2826–42.
12. Shahzad H et al. UV-spectrophotometric and spectroscopic observed Vachellia nilotica and Nigella sativa formulations regularized the histopathological and biochemical parameters during wound contraction. 2025. 88(1): pp. 4–16.
13. Akhtar MF et al. *Evaluation of biological potential of UV-spectrophotometric, SEM, FTIR, and EDS observed Punica granatum and Plectranthus rugosus extract-coated silver nanoparticles: A comparative study.* 2024. 87(3): pp. 616–627.
14. Mughal TA et al. Antibacterial and wound healing efficacy of silver nanoparticles synthesized from root bark of berberis lycium royle. 2024. 9(19): p. e202401292.
15. Ali F et al. Bactericidal and antioxidant potential of Moringa oleifera capped silver nanoparticles under varied conditions. 2023. 8(43): p. e202301889.
16. Abbas Z et al. Radical scavenging potential of spectrophotometric, spectroscopic, microscopic, and EDX observed zinc oxide nanoparticles from leaves, buds, and flowers extract of Bauhinia variegata Linn: A thorough comparative insight. 2024. 87(9): pp. 2121–33.
17. Zhuo Y, Zhao Y-G, Zhang YJM. Enhancing drug solubility, bioavailability, and targeted therapeutic applications through magnetic nanoparticles. 2024. 29(20): p. 4854.
18. Kamble P et al. *Nanofiber based drug delivery systems for skin: A promising therapeutic approach.* 2017. 41: pp. 124–133.
19. Ghafoor B et al. *Review of the fabrication techniques and applications of polymeric electrospun nanofibers for drug delivery systems.* 2018. 48: pp. 82–87.
20. Balusamy B et al. *Progress in the design and development of fast-dissolving electrospun nanofibers based drug delivery systems-A systematic review.* 2020. 326: pp. 482–509.
21. Tomar S et al. *Current approaches in nanofiber-based drug delivery systems: methods and applications.* 2023: pp. 39–71.
22. Alonso-Carrillo N et al. *Extraction of phenolic compounds from Satureja macrostema using microwave-ultrasound assisted and reflux methods and evaluation of their antioxidant activity and cytotoxicity.* 2017. 103: pp. 213–221.
23. Oskoueian E et al. Nanoliposomes encapsulation of enriched phenolic fraction from pistachio hulls and its antioxidant, anti-inflammatory, and anti-melanogenic activities. 2020. 37(1): pp. 1–13.
24. Altan A, Aytac Z, Uyar TJFH. Carvacrol loaded electrospun fibrous films from Zein and Poly (lactic acid) for active food packaging. 2018. 81: pp. 48–59.
25. Abbasalipourkabir R et al. *Toxicity of zinc oxide nanoparticles on adult male Wistar rats.* 2015. 84: pp. 154–160.
26. Moshfegh F et al. Crocus sativus (saffron) petals extract and its active ingredient, anthocyanin improves ovarian dysfunction, regulation of inflammatory

genes and antioxidant factors in testosterone-induced PCOS mice. 2022. 282: p. 114594.
27. Alara OR, Abdurahman NH. I.J.C.r.i.f.s. Ukaegbu. Extr Phenolic Compounds: Rev. 2021;4:200–14.
28. Sepahpour S et al. Comparative analysis of chemical composition, antioxidant activity and quantitative characterization of some phenolic compounds in selected herbs and spices in different solvent extraction systems. 2018. 23(2): p. 402.
29. Nurcholis W et al. Total flavonoid content and antioxidant activity of ethanol and Ethyl acetate extracts from accessions of Amomum compactum fruits. 2021. 66(1): pp. 58–62.
30. Deghima A et al. Anti-inflammatory activity of Ethyl acetate And n-butanol extracts from Ranunculus macrophyllus Desf. And their phenolic profile. 2021. 265: p. 113347.
31. Afsar T et al. *Antioxidant activity of polyphenolic compounds isolated from ethyl-acetate fraction of Acacia hydaspica R. Parker.* 2018. 12: pp. 1–13.
32. Minakov AV, et al. Rheological Prop Colloidal Suspensions Alumina Nanofibers. 2022;367:120385.
33. Luquis F et al. *Arctium lappa L.: Chemical composition, antioxidants, phytochemical compounds and use for healing activity.* 2021. 2(2): pp. 2063–2071.
34. Skowrońska W et al. *Arctium lappa and Arctium tomentosum, Sources of Arctii radix: Comparison of Anti-Lipoxygenase and Antioxidant Activity as well as the Chemical Composition of Extracts from Aerial Parts and from Roots.* 2021. 10(1): p. 78.
35. Carlotto J et al. *Polysaccharides from Arctium lappa L.: Chemical structure and biological activity.* 2016. 91: pp. 954–960.
36. Ferracane R et al. Metabolic profile of the bioactive compounds of Burdock (Arctium lappa) seeds, roots and leaves. 2010. 51(2): pp. 399–404.
37. Tsikas DJAb. *Assessment of lipid peroxidation by measuring malondialdehyde (MDA) and relatives in biological samples: Analytical and biological challenges.* 2017. 524: pp. 13–30.
38. Cordiano R et al. Malondialdehyde as a potential oxidative stress marker for allergy-oriented diseases: an update. 2023. 28(16): p. 5979.
39. Sabuncu T et al. Oxidative stress in polycystic ovary syndrome and its contribution to the risk of cardiovascular disease☆. 2001. 34(5): pp. 407–13.
40. Yifu PJBMG. Evidence for causal effects of polycystic ovary syndrome on oxidative stress: a two-sample Mendelian randomisation study. 2023. 16(1): p. 141.
41. Hu Q et al. Crocetin attenuates DHT-induced polycystic ovary syndrome in mice via revising Kisspeptin neurons. 2018. 107: pp. 1363–9.
42. Darabi P, Khazali H, Mehrabani MJGE, Natanzi. Therapeutic potentials of the natural plant flavonoid apigenin in polycystic ovary syndrome in rat model: via modulation of pro-inflammatory cytokines and antioxidant activity. 2020. 36(7): pp. 582–7.

Publisher's note